FLUORIDE

Quarterly Journal of The International Society for Fluoride Research Inc.

Algorithm-driven MRI Fetal Brain Disease Detection Image Processing Model Integrating Fluoride Exposure Risk Assessment: Public Health Perspective

Unique digital address (Digital object identifier [DOI] equivalent): https://www.fluorideresearch.online/epub/files/394.pdf

Qianqian WU, Yuankai CHEN, Zhenqing LIU, Fan WU, Hongsheng LIU*

Radiology Department, The Women and Children's Medical Center of Guangzhou Medical University, Yuexiu District, Guangzhou, 510120, China

* Corresponding author:

Dr. Hongsheng LIU, Radiology Department, The Women and Children's Medical Center of Guangzhou Medical University, Yuexiu District, Guangzhou, 510120, China

E-mail: liu15641@outlook.com

Submitted: 2025.07.25 Accepted: 2025.09.20 Published as e394: 2025 Sep 30

ABSTRACT

Purpose: In view of the strong empirical dependence of traditional fetal brain Magnetic Resonance Imaging (MRI) disease detection models, the difficulty in integrating key environmental risk factors, such as fluoride exposure for comprehensive assessment, and the lack of public health applicability.

Methods: This study innovatively proposes an algorithm-driven multimodal fusion model. First, a dual-channel input is constructed; then, dynamic gated fusion mechanism designed. Finally, an integrated classifier is used to achieve intelligent disease detection.

Results: Experiments shows that the Dice coefficient of the lateral ventricle of the proposed model in the high fluoride exposure group reaches 0.95. In terms of disease detection, the area under the curve (AUC) value of the model in the high exposure group is 0.953. In the high-risk subgroup, the disease detection rate of the model reaches 89.5%, and warning time advanced to 3.0 weeks. In addition, the verification in cross-regional samples shows that the accuracy of the model in different populations reaches 91.4%. **Conclusions:** These results shows that while improving detection performance, the model has significant public health promotion value, and suitable for fetal health monitoring and early intervention under high environmental risks.

Keywords: Public health; Disease detection; Fluoride exposure; Fetal brain MRI; Deep learning algorithm

INTRODUCTION

Fluoride (F) exposure is associated with problems in fetal brain development. The combined new data from the prospective Odense Children's Cohort with results from two previous birth cohort studies in Mexico and Canada to discussed the dose-effect relationship of F as developmental neurotoxicant at high exposures.¹ The potential health problems bγ long-term exposure of concentrations, especially the effects on cognitive function in children from pregnancy to 18 years of age, and relationship between F exposure and children's cognitive outcomes.² The dietary F intake during pregnancy was associated with neurodevelopment in young childrens in 103 mother-infant pairs in the Mexico City Progress Cohort. Higher concentration of F have been shown to be neurotoxic, the optimal exposure range may also pose risks to the developing brain.3

Fluoride exposure may lead to neuroadaptive changes in the central nervous system at the molecular and cellular levels associated with physical dependence by affecting neuroinflammation and neurodegeneration.4 The poisoning of F as a global public health problem, and the phenomenon that long-term excessive F exposure leads to F accumulation in the hippocampus and causes cognitive dysfunction. 5 The association of F exposure from different sources and doses, and neurological diseases in children and adolescents studies shown to related, clinical evidence remains controversial.⁶ The maternal urinary iodine concentration affects the relationship between maternal urinary F and intelligence in boys and girls. In animal studies, the combination of intrauterineF exposure and low iodine has greater negative effects on offspring learning and memory than either alone, but this has not been studied in children7.

Do et al.⁸ assessed the Australian population using the Wechsler Adult Intelligence Scale, version 4, to explore the potential effects of early F exposure on cognitive neurodevelopment in response to the ongoing debate on this issue and emphasized the need for high-quality scientific evidence. However, these approaches mostly focused on the single-aspect analysis and fail to fully integrate imaging features with environmental exposure risks.

To address the shortcomings of existing methods, some studies have attempted to incorporate physiological models and deep learning algorithms (DLA). To assess the main sources of groundwater contamination and non-carcinogenic risks of nitrate and F pollution to human health by using principal component analysis (PCA) and multi-layer perceptron artificial neural network.⁹ The effects of F exposure on pregnancy through a rat model, simulating the prepregnancy and pregnancy exposure conditions in endemic areas to explore the potential changes of F on placenta. However, most approaches failed to design dynamic and adaptable fusion mechanism, and therefore failed to deeply characterize the specific role of environmental risks on brain development.¹⁰

Traditional fetal brain MRI disease detection models mostly rely on empirical methods, which make it difficult to comprehensively consider environmental factors that affect fetal health, such as F exposure. These models usually lack the applicability from the public health perspective and cannot effectively assess the impact of environmental risk factors on fetal development. Therefore, how to integrate image features with environmental exposure information to achieve more accurate disease prediction has become an important direction for current research.

This article proposes an algorithm-driven dynamic fusion model, which uses a dual-channel input structure to extract fetal brain image features using an

improved deep learning network and quantify F exposure risk based on the physiologically based pharmacokinetic (PBPK) model. The innovation lies in the introduction of a dynamic gated fusion mechanism, which adaptively weights and fuses image and environmental risk information according to the confidence of image features and exposure risk level, thereby breaking through the limitations of traditional models and improving the accuracy and stability of disease detection. This model is not only applicable to different exposure risk groups, but also provides a feasible solution for early identification and intervention of diseases related to environmental risk factors.

MATERIAL AND METHODS

Three-dimensional Segmentation Network of Fetal Brain MRI

In this study, three-dimensional (3D) segmentation of fetal brain MRI images is one of the key steps in the disease detection model. To this end, an improved 3D U-Net architecture is adopted, and its architecture is shown in Figure 1.

This architecture is optimized to accurately extract the features of key brain structures in three-dimensional space, especially the subtle changes in the fetal brain images. Traditional 2D segmentation methods cannot fully utilize spatial information, while 3D U-Net can effectively utilize the spatial context of the image to improve the accuracy and robustness of segmentation. ¹¹ In order to quantify the segmentation accuracy, it applied the Dice coefficient as the core evaluation indicator, as shown in equation 1.

$$Dice(A,B) = \frac{2|A \cap B|}{|A|+|B|} \tag{1}$$

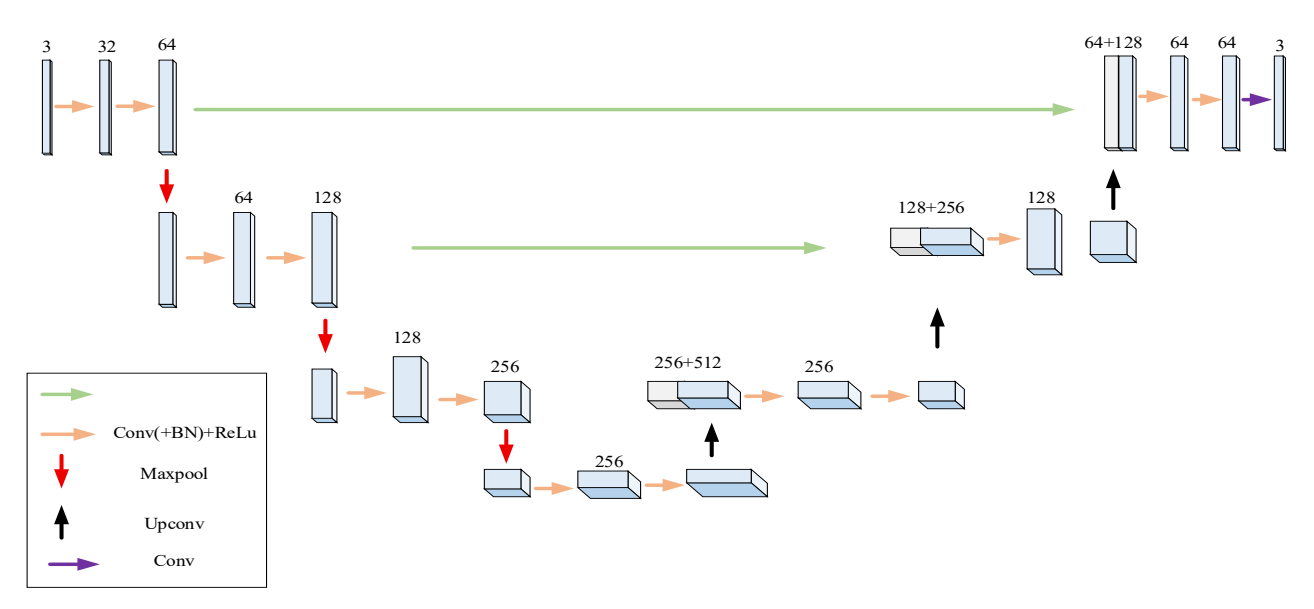


Figure 1. 3D U-Net network structure diagram

Table 1. The summary of the input indicators for the assessment of F exposure risk

Data type	Indicator	Unit	Collection method
Drinking water F	Water-F	mg/L	Regional average measurement
Urinary F	Urine-F	mg/L	Mid-gestation lab sample
Blood F	Blood-F	mg/L	Late-gestation lab sample
Exposure duration	Exposure time	Months	Questionnaire-based survey
Risk score	Composite risk index (R)	0–10 scale	Calculated via PBPK model

Among them, A represents the predicted segmentation area, and B represents the manually annotated real area. The core of this network structure is the encoder-decoder architecture, in which the encoder is used to extract high-level features of the image, and the decoder maps these features back to the original image size for accurate segmentation. In order to enhance the performance of the network, jump connections are added between the encoder and decoder, so that low-level detail features can be combined with high-level abstract features to further improve segmentation accuracy. In addition, spatial and channel attention mechanisms are integrated into the network so that the model can dynamically adjust the importance of features and automatically focus on those areas that have a greater impact on the segmentation results. In this way, the network can process complex fetal brain MRI images more efficiently, especially in the segmentation tasks of low-contrast areas and subtle lesions.

Fluoride Exposure Risk Quantification Module

The potential impact of F exposure on fetal brain development has not received sufficient attention, and this module provides important auxiliary information for disease detection models by quantifying F exposure risks. First, the multiple data sources are integrated, including maternal biological samples, i.e., blood and urine F concentrations, F concentration data of water sources in the place of residence, and duration of exposure during pregnancy. These data are obtained through laboratory testing and environmental monitoring, covering samples with different exposure levels. Based on these data, the PBPK model is used to calculate the F exposure risk score for each individual. Table 1 summarized the data used for exposure risk assessment in this study.

The PBPK model can simulate the absorption, distribution, metabolism and excretion of F in the body, thereby providing an accurate exposure level assessment for each subject. In order to enhance the accuracy of the exposure score, the exposure duration and environmental factors, i.e., F water source are further combined to quantify the exposure risk of each individual. The following equation is used for the quantification.

$$R_{score} = \alpha \cdot C_{urine} + \beta \cdot C_{blood} + \gamma \cdot C_{water}$$
 (2)

 $C_{urine,}C_{blood,}$ and C_{water} represents the concentrations of F in urine, blood, and water, respectively. α , β , and γ are normalized weight coefficients determined based on the PBPK model. In this way, this module can provide a personalized exposure risk assessment for each fetus, thereby providing more accurate risk prediction data for subsequent disease detection. 12

Key physiological parameters of the models, such as organ volumes and blood flow rates were referenced to population physiological data from pregnant women. Pharmacokinetic parameters, i.e., rate constants were calibrated and validated using fitted population data to ensure consistency between model predictions and actual biomonitoring data, such as urinary F levels. The final individual composite risk index was calculated based on the predicted target dose throughout pregnancy.

Multimodal Dynamic Feature Fusion Mechanism

In this study, multimodal dynamic feature fusion mechanism is proposed. The core of this fusion mechanism is the dynamic gate fusion unit (GFU). This design enables the model to flexibly select the optimal feature combination according to the characteristics of the input data, as better adapt to needs of different exposure risk groups. In order to improve the efficiency of the fusion process, GFU adopts an adaptive weighting mechanism to adjust the weights of each channel feature in real time by calculating the correlation and mutual information between features, as shown in equation 3.

$$F_{fusion} = \sigma (W_1 F_{ima} + W_2 F_{exp} + b) \tag{3}$$

 F_{img} is the image feature; F_{exp} is the exposure risk feature; W_1 and W_2 are learnable weights; b is the bias term; σ represents the activation function. The model can automatically adjust the focus under different risk environments to ensure the reasonable integration of image information and environmental exposure information. The proposed model in this study can not only make full use of the spatial features in the image information, but also effectively consider the potential impact of environmental risk factors on fetal brain development.

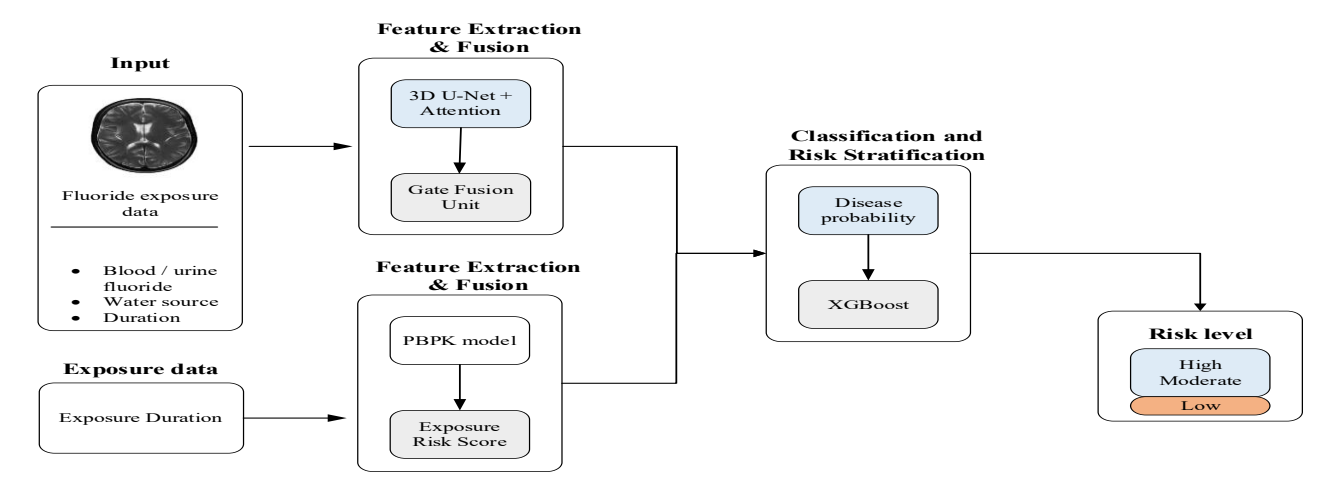


Figure 2. Disease classification and risk stratification module structure diagram

Disease Classification and Risk Stratification

Disease classification and risk stratification are one of the core links of the model, aiming to provide scientific basis for subsequent intervention measures by accurately identifying the type and risk level of fetal brain diseases. To achieve this goal, multimodal information, especially imaging data and F exposure risk data combined and advanced integrated classification algorithm is used for disease prediction and risk stratification. The model structure is shown in figure 2.

The input of the model includes feature data from the imaging-exposure dual channel. The imaging data is extracted through a deep learning network to extract the spatial characteristics of key brain structures, while the exposure risk data calculated through PBPK model to obtain a personalized F exposure risk score. According to the PBPK model, the individual exposure risk can be expressed as given equation.

$$R_{exposure} = \frac{C_{water} \cdot t_{exposure} \cdot V_{body}}{K_{body}}$$
 (4)

Where, $R_{exposure}$ is the individual F exposure risk; C_{water} is the F concentration in the water source; $t_{exposure}$ is the exposure duration; V_{body} is the volume factor; K_{body} is the metabolic constant. By fusing these two types of data, the comprehensive risk profile can be provided for each fetus.

The integrated classifier performs disease prediction after combining these two types of data. In order to improve the classification accuracy, the extreme gradient boosting (XGBoost) algorithm is used. As efficient integrated learning model, it can perform efficient feature selection and training in the multidimensional feature space. The loss function is shown in the equation 5.

$$L(\vartheta) = \sum_{i=1}^{n} [\log(1 + \exp(-y_i \cdot \hat{y_i}))] + \lambda \sum_{j=1}^{m} \vartheta_j^2$$
 (5)

Among them, $L(\vartheta)$ is the loss function; y_i is the true label; $\widehat{y_i}$ is the predicted output; λ is the regularization coefficient; ϑ_j is the model parameter. This classifier can not only classify diseases, but also stratify the risks of the fetus on this basis. Specifically, the model distinguishes high-risk groups from low-risk groups based on the patient's exposure risk level, providing more accurate disease warning information. 14

In terms of risk stratification, the model clearly divides high and low-risk groups by automatically grading the exposure score and combining the analysis results of imaging data. For example, the disease incidence rate of patients in the high-exposure group, such as blood F level>0.8 mg/L, water F concentration>1.5 mg/L is higher, and the model can identify this group in a timely manner and conduct key monitoring. Through this stratification, the model can provide accurate disease warning and early intervention measures for clinicians.

RESULTS AND DISCUSSION

Experimental Setting

Study Population and Data

This multicenter retrospective analysis used data from pregnancy cohort collected between January 2018 and December 2022 by six partner hospitals and local public health programs in three provinces in northern China. A total of 450 mother-fetus pairs were included. Inclusion criteria included singleton pregnancies, a well-defined brain MRI scan performed at approximately 24 weeks of pregnancy, both midpregnancy urine and blood F measurements, and complete records of F concentrations in residential water sources during pregnancy. Exclusion criteria included known genetic disorders, intrauterine infection, and severe motion artifacts on the MRI images.

Table 2. Describing the key specifications used in the model development

Category	Key Component	Configuration	
Hardware	GPU NVIDIA Tesla V100 (32GB)		
Dronronossina	Spatial normalization	1×1×1 mm³ isotropic resolution	
Preprocessing	Intensity correction N4 bias correction + Z-score		
2D II Not	Loss function	Dice + Weighted CE (3:1 ratio)	
3D U-Net	Batch size	4	
Fusion module	Gating unit	Dual-channel attentive GFU	
Fusion module	Weighting strategy	Risk-level adaptive	

Dataset

Source and Scale: This study collected fetal brain MRI data and related environmental and biological samples from multiple collaborating hospitals and public health programs. The sample size was estimated through statistical power analysis. Fluoride exposure stratification was based on the individual F exposure risk scores calculated from the PBPK model. The test set samples were divided into low, moderate and high-exposure groups. The following stratification thresholds were defined.

Low exposure group: R < 3.0 (corresponding to water F concentration < 0.7 mg/L, blood F concentration < 0.3 mg/L). Medium exposure group: $3.0 \le R \le 6.5$ (corresponding to water F concentration 0.7-1.5 mg/L, blood F concentration 0.3-0.7 mg/L). High exposure group: R > 6.5 (corresponding to water F concentration > 1.5 mg/L, blood F concentration > 0.7 mg/L). The test set contains 170 samples, divided into three groups, such as low exposure (n=68), medium exposure (n=68), and high exposure (n=34). This ensures balanced sample size across groups and facilitates performance comparison.

Comparative Model and Implementation

In order to highlight the advantages of this model incorporating environmental risk factors, the following baseline models are set for comparison, i.e., Baseline-1 (Group A)- single image model, Baseline-2 (Group B)-feature splicing model and present (Group C)- dynamic fusion model of this article. Table 2 summarizes the key implementation parameters, including hardware specifications, preprocessing standards, and fusion mechanisms.

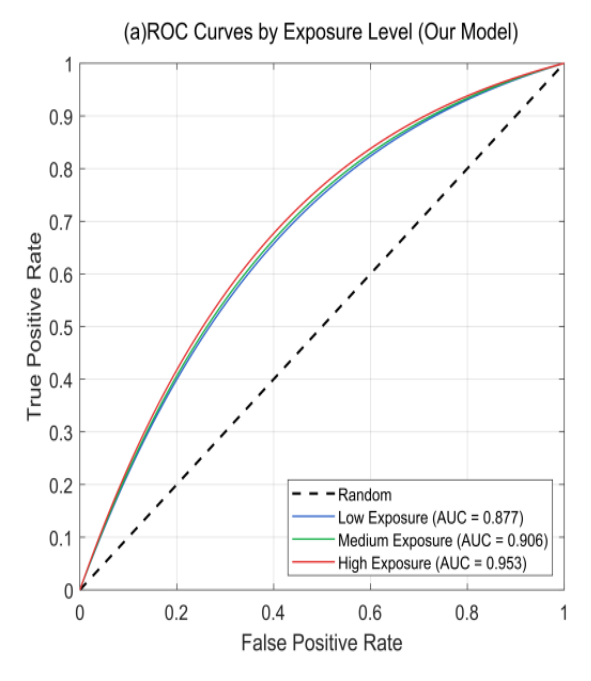
Segmentation Performance Experiment

This experiment aims to evaluate the impact of F exposure risk on the segmentation performance of key fetal brain structures. 60 stratified test samples (low/high/mixed exposure) are selected to compare three models, i.e., Group A (pure imaging model), Group B (feature splicing fusion), and Group C (dynamic gated fusion). Table 3 uses the Dice coefficient and Hausdorff distance (HD) as core indicators to quantify the differences in segmentation accuracy of the lateral ventricles and corpus callosum at different exposure levels, and explore the correlation between risk factors and anatomical structure recognition capabilities.

Table 3: The segmentation performance measurement of different brain structures at different F exposure

Brain structure	Model group	Exposure level	Dice	HD (mm)	Exposure sensitivity gain (ΔDice)	Inter-group p-value
Lateral ventricles	Group A	Low	0.88±0.04	2.8±0.7	0.07	-
		High	0.81±0.06	3.9±1.1	-0.07	
	Croup D	Low	0.89±0.03	2.7±0.6	0.05	-
	Group B	High	0.84±0.05	3.4±0.9	-0.05	
	Group C	Low	0.91±0.02	2.3±0.5	0.04	<0.001
		High	0.95±0.02	1.8±0.4	0.04	
Corpus callosum	Group A	Low	0.79±0.05	4.2±1.0	0.00	-
		High	0.70±0.07	5.6±1.4	-0.09	
	Group B	Low	0.80±0.04	4.0±0.9	0.06	-
		High	0.74±0.06	5.0±1.2	-0.06	
	Group C	Low	0.82±0.03	3.7±0.8	0.03	0.004
		High	0.85±0.03	3.1±0.6	0.03	

Note: Exposure-sensitive gain: Group C outperformed the low-exposure group in the high-exposure group (Δ Dice>0), demonstrating the models adaptability to risk groups. The high-exposure group's lateral ventricle Dice increased to 0.95 (95% CI: 0.94 - 0.96), statistically significant increase compared to Group A (p<0.001) (Wilcoxon test).



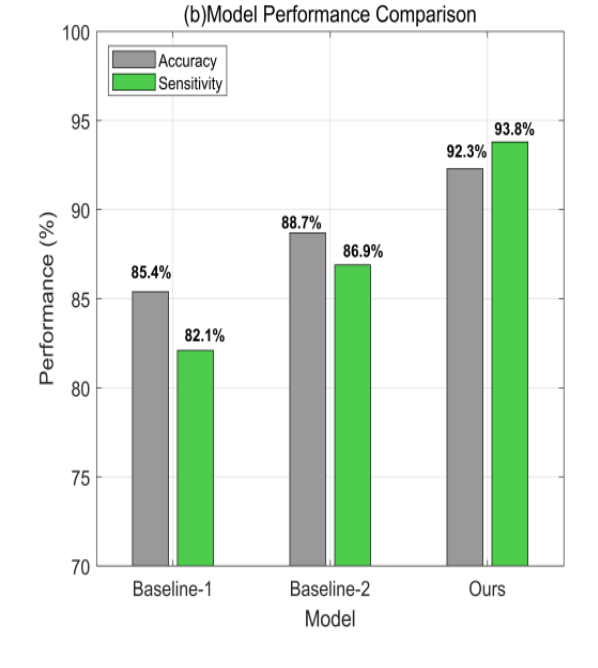


Figure 3. Disease detection evaluation

As can be seen from Table 3, taking the lateral example, the segmentation an performance of Group A/B in the high F exposure group significantly deteriorates the Dice coefficient of the lateral ventricle of Group A decreases from 0.88 ± 0.04 in the low exposure group to 0.81 ± 0.06 ($\Delta=$ -0.07), and HD increases from 2.8±0.7mm to 3.9±1.1mm. The model in this paper (Group C) reverses this trend through dynamic fusion mechanism. The Dice of the lateral ventricle in the high exposure group increases 0.95±0.02, the HD decreases 1.8±0.4mm; the exposure sensitivity gain ΔDice reaches +0.04. It is confirmed that the fusion exposure risk assessment can effectively suppress F interference and improve the robustness of anatomical structure recognition populations.

Disease Detection Evaluation Experiment

This experiment aims to assess the detection performance of fetal brain diseases under different F exposure levels. 170 stratified test samples (low/medium/high exposure groups) are applied to compare and analyze three models, such as single image model (Baseline-1), feature splicing model (Baseline-2) and the dynamic fusion model (present study). The three core indicators of accuracy, sensitivity and AUC are used to quantitatively verify the diagnostic performance of the model in different exposure risk environments, focusing on the detection stability of the high exposure group. The specific data are shown in Figure 3.

Figure 3a and b showed the ROC curves of the models under different exposure levels and comparison results of the three models in terms of

accuracy and sensitivity. The experimental results showed that the dynamic fusion model proposed in this paper is significantly better than traditional approach in disease detection performance. Among the 170 test samples, the overall accuracy of the model reaches 92.3% (Baseline-1: 85.4%, Baseline-2: 88.7%), and the sensitivity is 93.8% (Baseline-1: 82.1%, Baseline-2: 86.9%). As shown in Figure 3a, the AUC value of the model in the high exposure group reached 0.953 (95% CI: 0.932 - 0.974), which was significantly better than its performance in the medium exposure group (AUC=0.906, 95% CI: 0.876 - 0.936; DeLong's test, p=0.013) and the low exposure group (AUC=0.877, 95% CI: 0.842 - 0.912; DeLong's test, p<0.001). The specificity at each exposure level is maintained above 87%, indicating that the model can effectively avoid misdiagnosis while ensuring the disease detection rate. These data confirm that the fusion of F exposure risk assessment significantly improves the detection efficiency of fetal brain diseases, especially in the high-risk populations.

Risk Subgroup Experiment

This experiment focuses on the population with high F exposure risk (water F >1.5mg/L and blood F >0.8mg/L), and selects 38 confirmed encephalopathy cases from the test set as high-risk subgroup. By analyzing the dose-response relationship between exposure score and ventricular volume enlargement, Figure 4 and Table 4 assess the disease detection rate (HRDR) and warning lead time of different models for this subgroup, aiming to verify the early warning effectiveness of the fusion exposure risk assessment mechanism for high-risk populations.

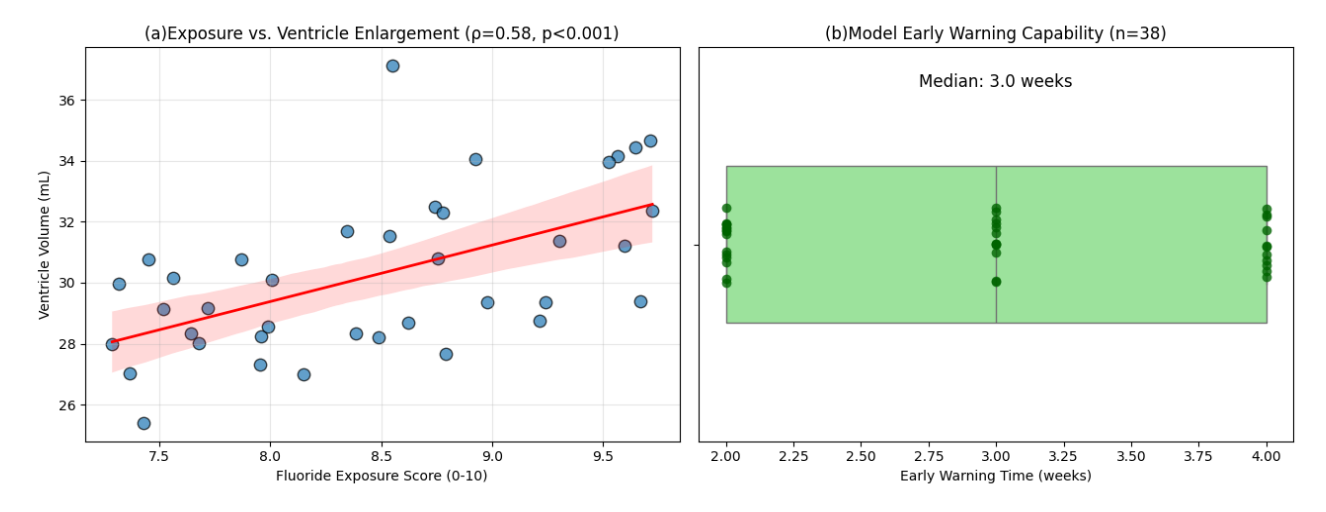


Figure 4. High-risk subgroup analysis

Table 4. The comparative performance of high-risk subgroup models

Model	HRDR (%)	Sensitivity (%)	Early warning lead time (weeks)	p-value vs. present
Baseline-1	71.1	76.3	1.8 ± 0.9	<0.001
Baseline-2	78.9	82.6	2.3 ± 1.1	0.018
Present study	89.5	94.7	3.0 ± 1.4	_

Fluoride exposure score is significantly positively correlated with the ventricular volume (Spearman p=0.58, p<0.001), and each increase of 1 unit in the exposure score leads to an increase of about 1.6 mL in the ventricular volume (Figure 4a). As shown in Table 4, the disease detection rate (HRDR) of the proposed model in the high-risk subgroup reaches 89.5, an increase of 18.4% compared with Baseline-1. The sensitivity is 94.7%, and the median warning time window 3.0 weeks (Figure 4b), which is earlier than the baseline model. The results confirmed that the fusion exposure risk assessment mechanism significantly improves the early warning efficiency of high-risk populations.

Model Generalization Ability Experiment

This experiment aims to evaluate the performance of different models for disease detection in high-risk populations. The data for this study is divided into two parts:

The Internal Training and Tuning Cohort consists of 380 samples from three core partner hospitals (e.g., Province A). All data were acquired using the same Siemens Skyra 3T scanner and standardized T2-weighted sequences for model training and initial validation.

The External Validation Cohort is used to test the model's generalization ability. This dataset consists of 300 samples intentionally selected from sources that differ significantly from the Internal Cohort:

Geographic and Institutional Differences: From two local hospitals and public health program.

Scanning Equipment Differences: Scanners range from the General Electric (GE) Discovery MR750 3T to the Philips Achieva 1.5T.

Imaaina Protocol Differences: Sequence parameters, such as TR/TE and voxel size exhibit natural variation. Demographic characteristics, i.e., mean maternal age and gestational age distribution differ slightly from the internal dataset. We tested model performance on external validation set, which differs significantly from the internal training set in scanner model, imaging parameters, and geographic origin. We analyzed the performance of each model across different exposure levels using metrics, such as accuracy, sensitivity, AUC, and HRDR, focusing on detection stability and early warning efficacy in the high-exposure group. Specific data are shown in Figure 5.

The experimental results showed that the dynamic fusion model has excellent generalization ability in different regions and groups. Among 300 fetal brain MRI samples from urban and rural areas, the model has an accuracy of 91.4%, sensitivity of 93.2%, and an AUC of 0.95 on the test set, which are significantly better than Baseline-1 (accuracy 84.3%, sensitivity 75.1%, AUC0.84) and Baseline-2 (accuracy 86.2%, sensitivity 79.4%, AUC0.87). In addition, the performance difference between the model in urban and rural samples are less than 2.3%, further proving its stability and reliability on different data sets. These results verify the wide applicability of the model and provide support for large-scale promotion.

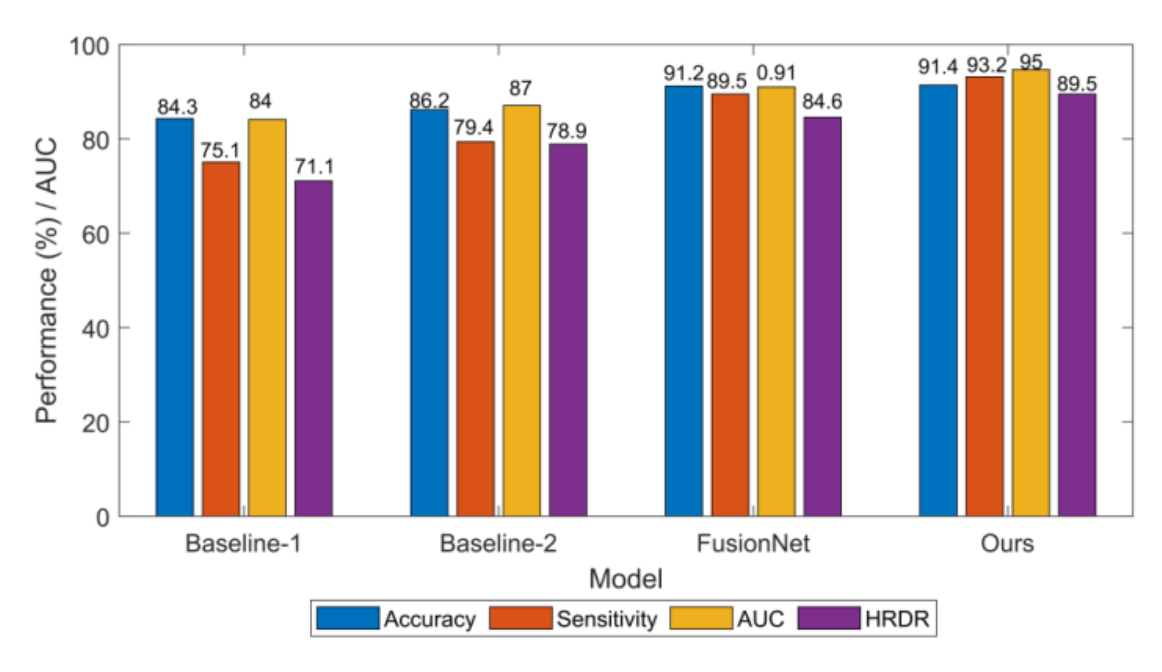


Figure 5. Model generalization ability evaluation

Significance of the Experimental Analysis

In this study, we proposed a fetal brain disease detection model based on the dynamic fusion mechanism and validated its performance through multiple experiments. Results showed that dynamic fusion model demonstrated significant advantages over traditional models in the high-F exposure group. Notably, this performance improvement may not only be due to algorithmic innovation but also relates to the biological mechanisms of F exposure. Existing research suggests that the F may induce subtle structural or signal changes in the brain by inducing neuroinflammation or affecting myelination. These changes, while difficult to detect visually, may be captured by deep learning models. Our dynamic gating mechanism, bγ incorporating exposure information, may enhance the model's sensitivity to these specific imaging features, thereby achieving more accurate detection in high-exposure groups.

In disease detection evaluation, our model achieved the highest AUC value in the high-exposure group, indicating that incorporating environmental risk factors can significantly improve screening efficacy in high-risk populations. However, the clinical application of any diagnostic tool requires careful assessment of the risk of false positives. False-positive results may lead to unnecessary anxiety and subsequent invasive testing for pregnant women, while false-negative results may delay intervention. Therefore, in future clinical translation, this model is more suitable as auxiliary screening tool, combined with expert assessment, and by setting a higher decision threshold to balance detection rate and false positive rate. The model's generalization ability was validated in heterogeneous dataset across regions and

multiple scanning devices, with performance degradation below 1%, demonstrating its robustness. Finally, risk subgroup analysis confirmed the model's early warning value for high-risk populations.

It is important to note that this study still has several limitations. As an observational study, although exposure was quantified using PBPK model and some covariates were adjusted, the influence of other confounding factors, such as socioeconomic status, nutrition, and co-exposure to other toxicants cannot be fully excluded. Furthermore, the clinical integration of the model requires further exploration, including cost-effectiveness analysis and how risk scores can be translated into clinical intervention strategies. In summary, this study not only proposes an effective algorithmic framework but also provides new insights for exploring the imaging associations environmental toxicants development. Its clinical applicability awaits further validation in prospective cohorts.

CONCLUSIONS AND FUTURE RESEARCH GAP

Fetal brain disease detection model based on the dynamic fusion mechanism proposed in this paper successfully combines imaging features with F exposure risk information, significantly improving the accuracy of disease detection and early warning capabilities. Through experimental verification, the model performs well in high-risk groups, especially in terms of disease detection rate and sensitivity, which is superior to traditional models, and can provide effective warning time in advance. In addition, the model has strong generalization ability, and the application effect in different regions and groups are stable. Despite this, this study still has specific

limitations, mainly in terms of sample size and diversity, and its performance needs to be further verified in a larger range and more complex environment in the future. Future research can further optimize the computational efficiency of the model and explore more potential associations between environmental factors and diseases to enhance the practical application value of the model, especially for its widespread promotion in the field of public health.

FUNDING

This work was supported by the Science and Technology Projects in Guangzhou (202201020630, 202201020627).

DISCLOSURE OF FINANCIAL AND NON-FINANCIAL RELATIONSHIPS AND ACTIVITIES AND CONFLICTS OF INTEREST

None

REFERENCES

- [1] Grandjean P, Meddis A, Nielsen F, Beck IH, Bilenberg N, Goodman CV, et al. Dose dependence of prenatal fluoride exposure associations with cognitive performance at school age in three prospective studies. Eur J Public Health 2024;34(1):143-9. DOI: 10.1093/eurpub/ckad170.
- [2] Gopu BP, Azevedo LB, Duckworth RM, Subramanian MKP, John S, Zohoori FV. The relationship between fluoride exposure and cognitive outcomes from gestation to adulthood—a systematic review. Int J Environ Res Public Health 2022;20(1):22-31. DOI: 10.3390/ijerph20010022
- [3] Cantoral A, Téllez-Rojo MM, Malin AJ, Schnaas L, Osorio-Valencia E, Mercado A, et al. Dietary fluoride intake during pregnancy and neurodevelopment in toddlers: a prospective study in the progress cohort. Neurotoxicology 2021;87(1):86-93. DOI: 10.1016/j.neuro.2021.08.015
- [4] Kupnicka P, Listos J, Tarnowski M, Kolasa A, Kapczuk P, Surowka A, et al. The effect of prenatal and neonatal fluoride exposure to morphine-induced neuroinflammation. Int J Mol Sci 2024;25(2):826. DOI: 10.3390/ijms25020826
- [5] Zhang Y, Gao Y, Liu X. Focus on cognitive impairment induced by excessive fluoride: An update review. Neuroscience 2024;558(1):22-9. DOI: 10.1016/j.neuroscience.2024.08.011
- [6] Miranda GHN, Alvarenga MOP, Ferreira MKM, Puty B, Bittencourt LO, Fagundes NCF, et al. A systematic review and meta-analysis of the association between fluoride exposure and neurological disorders. Sci Rep 2021;11(1):22659. DOI: 10.1038/s41598-021-99688-w
- [7] Goodman CV, Hall M, Green R, Chevrier J, Arotte P, Martinez-Mier EA, et al. Iodine status modifies the association between fluoride exposure in pregnancy and preschool boys' intelligence. Nutrients 2022;14(14):2920. DOI: 10.3390/nu14142920
- [8] Do LG, Sawyer A, Spencer AJ, Leary S, Kuring JK, Jones AL, et al. Early childhood exposures to fluorides and cognitive neurodevelopment: a population-based longitudinal study. J Dent Res 2025;104(3):243-50. DOI: 10.1177/00220345241299352

- [9] Mohammed MAA, Mohamed A, Szabó NP, Szucs P. Development of machine-learning-based models for identifying the sources of nitrate and fluoride in groundwater and predicting their human health risks. Int J Energ Water Res 2024;8(2):161-180. DOI: 10.1007/s42108-023-00271-y
- [10] Guerrero-Arroyo J, Jiménez-Córdova MI, Aztatzi-Aguilar OG, Razo LMD. Impact of fluoride exposure on rat placenta: foetal/placental morphometric alterations and decreased placental vascular density. Biol Trace Elem Res 2024;202(7):3237-47. DOI: 10.1007/s12011-023-03916-5
- [11] Chen J, Cheng A, Xia C, Qiu B. Investigating the mental health implications of AIGC education and fluoride consumption among college students. Fluoride 2024;e299. https://www.fluorideresearch.online/epub/files/299.pdf
- [12] Kumar JV, Moss ME, Liu H, Fisher-Owens S. Association between low fluoride exposure and children's intelligence: a meta-analysis relevant to community water fluoridation. Public Health 2023;219:73-84. DOI: 10.1016/j.puhe.2023.03.011
- [13] Do LG, Spencer AJ, Sawyer A, Jones A, Leary S, Roberts R, et al. Early childhood exposures to fluorides and child behavioral development and executive function: a population-based longitudinal study. J Dent Res 2023;102(1):28-36. DOI: 10.1177/00220345221119431
- [14] Singh A, Sharma A, Agrawal M, Sundaram S. Fluoride: toxicity, mechanism and role of bioremediation in detoxification. Curr Microbiol 2025;82(8):372. DOI: 10.1007/s00284-025-04365